# LANGMUIR

pubs.acs.org/Langmuir Article

# Model Asphaltenes Adsorbed onto Methyl- and COOH-Terminated SAMs on Gold

Thaddeus W. Golbek, Ryan A. Faase, Mette H. Rasmussen, Rik R. Tykwinski, Jeffrey M. Stryker, Simon Ivar Andersen, Joe E. Baio, and Tobias Weidner\*



Cite This: Langmuir 2021, 37, 9785-9792



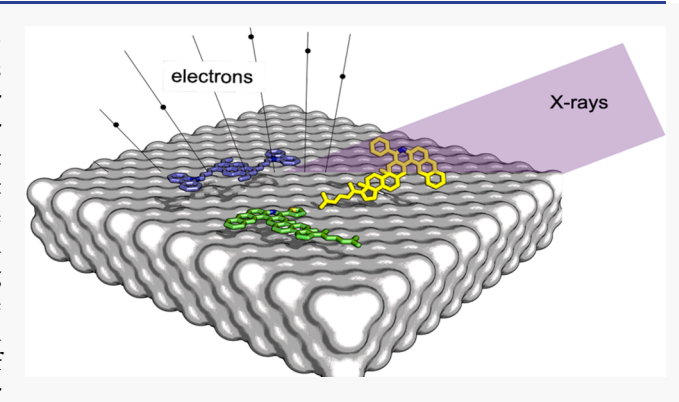
**ACCESS** I

III Metrics & More



SI Supporting Information

ABSTRACT: Petroleum asphaltenes are surface-active compounds found in crude oils, and their interactions with surfaces and interfaces have huge implications for many facets of reservoir exploitation, including production, transportation, and oil—water separation. The asphaltene fraction in oil, found in the highest boiling-point range, is composed of many different molecules that vary in size, functionality, and polarity. Studies done on asphaltene fractions have suggested that they interact via polyaromatic and heteroaromatic ring structures and functional groups containing nitrogen, sulfur, and oxygen. However, isolating a single pure chemical structure of asphaltene in abundance is challenging and often not possible, which impairs the molecular-level study of asphaltenes of various architectures on surfaces. Thus, to further



the molecular fundamental understanding, we chose to use functionalized model asphaltenes (AcChol-Th, AcChol-Ph, and 1,6-DiEtPy[Bu-Carb]) and model self-assembled monolayer (SAM) surfaces with precisely known chemical structures, whereby the hydrophobicity of the model surface is controlled. We applied solutions of asphaltenes to these SAM surfaces and then analyzed them with surface-sensitive techniques of near-edge X-ray absorption fine structure (NEXAFS) and X-ray photoelectron spectroscopy (XPS). We observe no adsorption of asphaltenes to the hydrophobic surface. On the hydrophilic surface, AcChol-Ph penetrates into the SAM with a preferential orientation parallel to the surface; AcChol-Th adsorbs in a similar manner, and 1,6-DiEtPy[Bu-Carb] binds the surface with a bent binding geometry. Overall, this study demonstrates the need for studying pure and fractionated asphaltenes at the molecular level, as even within a family of asphaltene congeners, very different surface interactions can occur.

#### INTRODUCTION

Petroleum asphaltenes are important surface-active components of heavy crude oil, and their ability to interact at and with surfaces such as minerals, pipe walls, oil—water interfaces, and catalysts has economic and environmental implications for reservoir drainage, production, oil-water separation, transportation, and refinery operations. 1,2 Asphaltenes are operationally defined as material precipitating upon the addition of excess *n*-alkanes (e.g., *n*-heptane is the standard precipitant), and this precipitate can be dissolved in toluene. 1,2 As such, the asphaltene fraction is composed of innumerable unique molecules that vary in size, functionality, and polarity, related only by the low solubility in the defining alkane as well as the apparent and abundantly researched ability to interact and "self-associate". Asphaltenes are found both in the highest boiling-point range of the oil (vacuum residue, bp  $\leq 600$  °C) and in the nondistillable, higher-molecular-weight constituents, the so-called petroleum heavy ends. There is a severe economic impact of asphaltenes over the entire oil and gas industry, with numerous studies performed to identify and

classify asphaltenes in terms of specific molecular structures and functionality that may explain the observed physical phenomenon and mitigate the problems.

Various phenomena during oil production are related to the adhesion of oil components to surfaces and interfaces. In these processes, both the wettability of the surface and the enthalpy of adhesion are important. Herein, we illustrate this on a model scale using model asphaltene molecules *and* model surfaces. Distinct differences are noted.

The impact of asphaltenes at material surfaces has been studied for decades, but there is still surprisingly little known about the interaction of asphaltenes with material surfaces at the molecular level. This lack of information is due to the

Received: May 19, 2021 Revised: July 19, 2021 Published: August 5, 2021





challenge of isolating specific asphaltenes from crude oil mixtures and the general difficulty of probing the molecular structure within molecular monolayers. Acevedo et al. have used many techniques, such as Fourier transform ion cyclotron resonance mass spectrometry (FT-ICR MS), to study the structure of unfractionated asphaltene samples and its relation to precipitation of the process.<sup>4</sup> They found that smaller asphaltenes form more organized structures and suffer less deposition than the larger "archipelago" constituents, which form less-organized structures with a greater amount of deposition. Andrews et al. have studied asphaltenes at the air-water interface using sum frequency generation spectroscopy. Sauerer et al. showed that the adsorption of asphaltenes from crude oil at the oil-water interface leads to a fractionation of the asphaltenes—hence, molecular properties of the bulk phase asphaltenes are different from those found at the interface.<sup>6</sup> While experiments at water surfaces are important for technical applications involving bitumen-mineral emulsions and the chemistry of the production water, structural data about asphaltenes at solid material surfaces are extremely important for oil recovery, transportation, and production surfaces. To date, numerous studies utilizing atomic force microscopy (AFM) have been conducted on asphaltenes adsorbed onto solid surfaces.<sup>7–11</sup> Despite numerous studies of asphaltene adsorption from solution onto solid surfaces, the exact nature of these interactions remains speculative, due to the complexity of asphaltenes and the potential for preferential adsorption of certain molecular families over others. To further our fundamental understanding, another approach is needed, one that avoids the use of a mixture of natural asphaltene materials of different origins. Equally important is the use of surfaces with a precisely known chemical structure and properties, allowing specific interactions to be identified, evaluated, and quantified.

Asphaltenes reportedly interact with other substances via poly- and heteroaromatic ring structures as well as functional groups containing nitrogen, sulfur, and oxygen. The identification of such functional groups, as well as an abundance of mass spectrometric data, provides the natural abundance and distributions of nitrogen-, sulfur-, and oxygen-containing compounds (NSO types). Schuler et al. have provided new knowledge of individual molecular structures in petroleum heavy ends using AFM. 12-16 Although, these works provide and confirm indirect knowledge of various structural features, including aromaticity, functional groups, and positioning of alkyl side chains, they cannot be isolated in abundance, preventing a determination of the impact of various molecular architectures and functionality on surface behavior. Because of the lack of "pure" asphaltene molecules that can be used in fundamental studies, several lines of model asphaltene molecules have been constructed. 17 Synthetic model compounds that faithfully mirror the asphaltene structure and functionality can provide molecular-level insight into how and why the asphaltenes possess unique, peculiar properties, including aggregation behavior and thermal chemistry.

In this study, we determine the interaction of three model asphaltenes, AcChol-Th, AcChol-Ph, and 1,6-DiEtPy[Bu-Carb] (Figure 1), at hydrophobic and hydrophilic model surfaces using X-ray photoelectron spectroscopy (XPS) and near-edge X-ray absorption fine structure (NEXAFS) spectroscopy. The molecular architecture of the species was selected primarily to represent nitrogen-containing compounds. AcChol-Th and AcChol-Ph have similar asymmetric

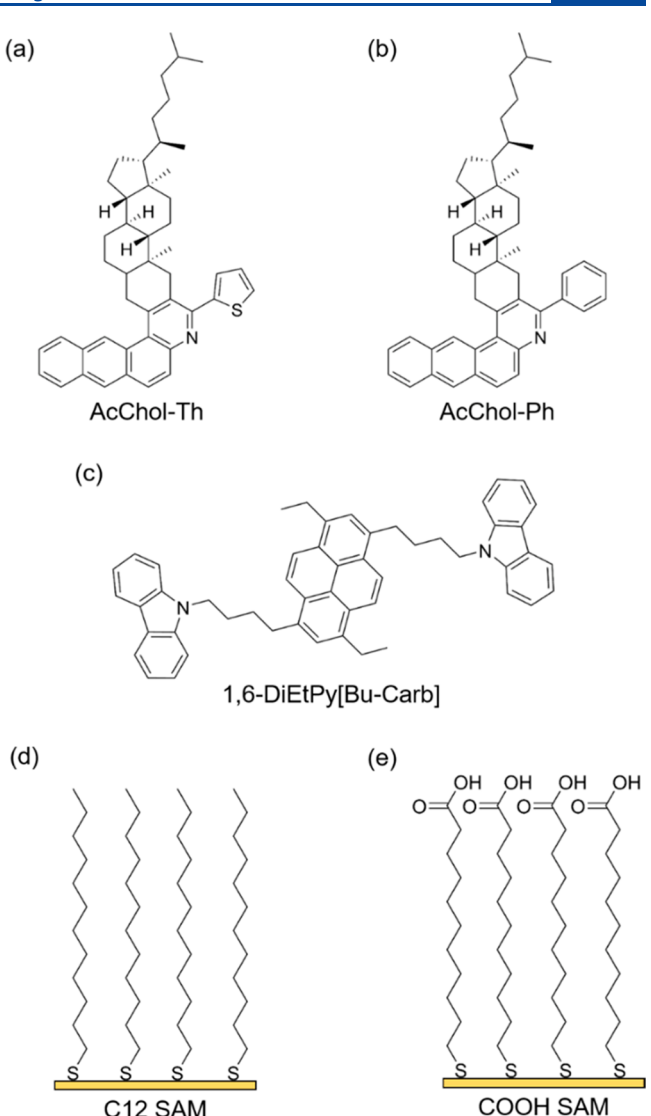


Figure 1. Structures of the asphaltene model compounds in this study (AcChol-Th, AcChol-Ph, and 1,6-DiEtPy[Bu-Carb]) and the structure of the self-assembled monolayer (SAM) surfaces (C12 and COOH).

C12 SAM

"naphthenic" hydrocarbon structures fused to a naphthoquinone aromatic moiety, differing only in the appended aromatic ring:  $\alpha$ -thiophenyl and phenyl. The other structure, 1,6-DiEtPy[Bu-Carb], is a C<sub>2</sub>-symmetric "archipelago structure" with two pendant alkyl carbazole moieties tethered to the central pyrene via saturated four-carbon linkers. Utilizing XPS, the elemental composition of an asphaltene film and the amount of material adsorbed can be determined, while NEXAFS spectra interrogate the order and orientation of adsorbate species. As mentioned, we also selected model surfaces to mimic either a hydrophobic "oily" surface or one that interacts mainly through hydrogen bonding but retains a largely oily surface, i.e., hydrophytic. For model surfaces, we prepared self-assembled monolayers (SAMs) on gold. SAMs can be used to fabricate reproducible and consistent model systems where the surface polarity, charge, and chemical identity can be tailored by changing the chemistry of the SAM functional group. Hydrophobic surfaces were prepared using 1dodecanthiol (C12) with methyl terminal groups, and hydrophilic surfaces were prepared by using 11-mercaptoundecanoic acid (COOH), which carries a terminal carboxylic acid group. XPS and NEXAFS spectra show that the binding of asphaltenes is strongly affected by the surface chemistry.

# **■ EXPERIMENTAL SECTION**

**Model Compounds.** Samples of AcChol-Th, <sup>19</sup> AcChol-Ph, <sup>19</sup> and 1,6-DiEtPy[Bu-Carb]<sup>20</sup> were synthesized as previously described.

Sample Preparation. Silicon wafer substrates  $(1 \times 1 \text{ cm})$  were cleaned by soaking in Milli-Q water overnight followed by rinsing with Milli-Q water and then acetone the next morning. The silicon substrates were then further cleaned by sonication sequentially in DCM (dichloromethane), acetone, and ethanol and then dried under a stream of nitrogen and stored until E-beam deposition [Polyteknik explorer 500 GLAD (glancing angle deposition) e-beam deposition system, 0° tilt angle, no rotation]. Substrates were prepared by Ebeam deposition of 4 nm of titanium (Kurt J. Lesker, 99.995% pure) followed by 100 nm of gold (Dansk Ædelmetal, GU1119, 99.999% pure) onto a clean silicon wafer. Gold-coated wafers were immersed in ethanoic solutions of 1 mM 1-dodecanthiol (C12, Sigma-Aldrich) or 2 mM 11-mercaptoundecanoic acid (COOH, Sigma-Aldrich). The samples were backfilled with nitrogen, sealed with parafilm, and stored in the absence of light for 24 h. After 24 h, the samples were thoroughly washed with ethanol and dried under nitrogen.

For the adsorption of model asphaltene compounds, 0.2% w/w solutions were made by dissolving the compounds AcChol-Th, AcChol-Ph, and 1,6-DiEtPy[Bu-Carb] in toluene. The prepared solutions were set on a shaker overnight (16 h). The prepared SAMs of C12 and COOH were then submerged in the prepared asphaltene solutions for 10 h. The SAMs were then washed with toluene, dried with nitrogen, and stored until the surfaces could be analyzed.

X-ray Photoelectron Spectroscopy (XPS). XPS experiments were performed on a Kratos AXIS Ultra DLD instrument equipped with a monochromatic Al K $\alpha$  X-ray source ( $h\nu = 1486.6$  eV, 300 W, 15 kV). All spectra were collected in hybrid mode at a takeoff angle of 0° (angle between the sample surface plane and the axis of the analyzer lens) and corrected to the Au 4f<sub>7/2</sub> emission of the underlying gold substrate at 83.95 eV, and a linear background was subtracted for all peak area quantifications. An analyzer pass energy of 160 eV was used for compositional survey scans of C 1s, O 1s, S 2p, and Au 4f. High-resolution scans of C 1s and S 2p elements were collected at an analyzer pass energy of 20 eV (energy resolution <0.7 eV). Error in the reported data is calculated by the standard deviation of the atomic percent average of the three spots. The peak areas were normalized by the sensitivity factors provided by the manufacturer, and the surface compositions and fits of the high-resolution scans were calculated in CasaXPS (Casa Software Ltd.).

The amount of adsorbed asphaltenes on the surface of the SAMs can be followed by the carbon atomic percent determined from the C 1s signal. Here, we are interested in knowing the carbon amount of just the overlayer, which will allow calculation of the thickness of the asphaltenes adsorbed to the surface of the SAMs. Since the SAM substrate contains carbon, the contribution of the C 1s from the underlying SAM layer must be removed in order determine the asphaltene layer thickness. Thus, the carbon from just the asphaltene layer can be calculated by examining the attenuation of the Au 4f signal from the surface of the gold substrates after asphaltene adsorption to the surface by eq 1.<sup>21,22</sup>

$$C_{\text{norm}} = C_{\text{o}} - C_{\text{s}} (Au_{\text{o}}/Au_{\text{s}})$$
 (1)

where s denotes the SAM substrate; o denotes the asphaltene overlayer;  $C_{\rm s}$  and  ${\rm Au}_{\rm s}$  are the measured C 1s and Au 4f atomic percent, respectively, from either the COOH or C12 SAM on gold prior to asphaltene adsorption;  $C_{\rm o}$  and  ${\rm Au}_{\rm o}$  are the measured C 1s and Au 4f, respectively, from the SAM on the gold substrate after asphaltene adsorption; and  $C_{\rm norm}$  is the C 1s atomic percent that accounts for just the adsorbed asphaltenes.

Next, by utilizing the fact that elemental gold is only found in the substrates and not in the surface overlayer, we can use it to estimate

the thickness of the adsorbed as phaltenes. Equation 2 was used to determine the overlayer thickness:  $^{23-25}$ 

$$I_{\text{overlayer}} = I_{\text{substrate}} e^{(-d/\lambda \cos \theta)} \tag{2}$$

where I is the flux of the electrons, d is the overlayer thickness,  $\lambda$  is the density of the advantageous carbon (a reasonable assumption that is similar to the theoretical carbon overlayer in the adsorbed asphaltenes), and  $\theta$  is the photoelectron takeoff angle. A density of 1.1 g/cm<sup>3</sup> was assumed.<sup>22</sup>

Near-Edge X-ray Absorption Fine Structure Spectroscopy. Carbon K-edge near-edge X-ray absorption fine structure (NEXAFS) spectra were collected at the 7-ID-1 SST-1 beamline at the National Synchrotron Light Source II (NSLS II, Brookhaven National Laboratory, Upton, NY) using an elliptically p-polarized (~85%) beam. The beamline is equipped with a monochromator and a 1200 L/mm grating that provides a full-width at half-maximum resolution of better than 0.1 eV at the carbon K-edge (285 eV). The monochromator energy scale was calibrated using the 285 eV C 1s  $\rightarrow \pi^*$  transition on a graphene grid while partial electron yields were divided by the beam flux of a gold grid during data acquisition. A detector with a bias voltage of -150 V monitored partial electron yields. All samples were mounted to allow rotation about the vertical axis, thus allowing the NEXAFS angle, the angle between the incident X-ray beam and the sample surface, to change. Previously, we ruled out the possibility of beam damage by repeatedly scanning between the 280-290 eV energy range while monitoring the partial electron yield at 285 eV. No changes in the spectra were observed within 15 min, which exceeded the exposure time in the longest carbon scan.

# RESULTS AND DISCUSSION

NEXAFS Analysis of Asphaltenes Interacting with C12 and COOH SAMs. The structure of the model asphaltenes when bound to hydrophobic and hydrophilic SAMs was probed by NEXAFS spectroscopy. Carbon K-edge spectra recorded at 90° and 20° for asphaltenes bound to COOH SAMs are presented in Figure 2. The neat COOH spectrum displays all expected resonances for a mercaptoundecanoic acid SAM.  $^{26}$  A sharp resonance near 288 eV and a shoulder near 286 eV can be assigned to a convolution of  $\pi^*C$ =O and  $\sigma^*C$ —H transitions.  $^{27,28}$  Broader resonances at higher photon

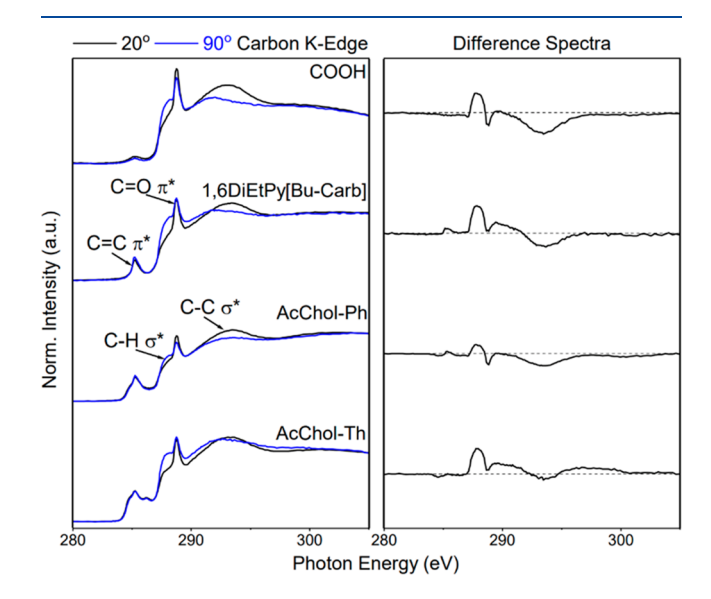


**Figure 2.** (left) NEXAFS spectra recorded at  $90^{\circ}$  and  $20^{\circ}$  X-ray incidence angles for COOH SAM with and without exposure to asphaltene model compounds. (right) Difference between the  $90^{\circ}$  and  $20^{\circ}$  NEXAFS spectra.

energies can be assigned to C—C and C—O moieties within the SAMs. A very weak peak at  $\sim$ 285.2 eV is also observed. This peak is tentatively assigned to an excitation into alkane—substrate orbitals. <sup>29,30</sup>

Angle-dependent variations of the spectral intensities, the so-called linear dichroism of X-ray absorption, is an effective probe of molecular alignment. The positive dichroism observed for the C—H resonance and the corresponding negative dichroism for the C—C transitions, also highlighted in the difference spectra (Figure 2), clearly show that, as expected, the COOH SAMs are well-aligned and the chains oriented upright. The strong negative feature related to the terminal carboxyl group shows that the C=O bond is pointing away from the surface and aligned with the alkyl chains.

Upon exposure to model asphaltenes, all COOH SAM spectra exhibit a significant  $\pi^*C$ =C resonance near 285 eV related to the aromatic bonds. AcChol-Th shows an additional shoulder near 285.5 eV, likely related to the thiophene ring. Since COOH SAMs do not contain aromatic groups, this clearly shows the presence of asphaltenes on the SAM surfaces.

The intensity of the  $\pi^*C=O$  feature decreases for all COOH SAM/asphaltene assemblies, which indicates that the relative amounts of molecules at the surface without C=O bonds have increased, again confirming asphaltene binding. Interestingly, the dichroism related to the C=O bonds is also significantly reduced. The disturbance of the order of the carboxyl groups at the SAM surface is direct evidence for interactions of asphaltenes with the outermost SAM region, such as intercalation, steric repulsion, and charge interactions. The dichroism related to the C—H moieties remains largely unchanged for 1,6-DiEtPy[Bu-Carb] and AcChol-Th SAM, but it is reduced for binding the AcChol-Ph model asphaltene—a clear indication that the phenyl functionality disturbs the order of the alkyl chains, likely by penetrating partly into the SAM structure.

There is only a small dichroism observable for the aromatic systems associated with asphaltenes. This can be explained by a combination of an inhomogeneous orientation of asphaltenes on the surface and the inherent distribution of the orientations of the aromatic system within the asphaltene molecules. For 1,6-DiEtPy[Bu-Carb], a weak positive dichroism is detected, which indicates a slight predominance of ring-plane orientations perpendicular to the surface. AcChol-Th, on the other hand, displays a weak negative dichroism for the preedge  $\pi^*$  resonance, which points to a more flat adsorption geometry of the ring planes.

The spectra for C12 SAM with and without exposure to model asphaltene compounds in Figure 3 show all expected transitions for an alkyl thiol SAM on gold: a narrow feature near 286 eV is assigned to C-H moieties, and the broader  $\sigma^*C-C$  resonances are also observed. The spectral dichroism is indicative of a well-aligned alkanethiol SAM with an upright orientation: a positive dichroism for the C-H-related peaks in combination with a negative feature for the C-C bonds. 31-33 After exposure to the asphaltene solutions, the spectra remain virtually unchanged. No additional surface species are detected, and the SAM structure is not affected by the interaction with the asphaltene solution. The NEXAFS results would have revealed any disturbance of the alkane chains by asphaltene interaction. Based on the fact that the SAM spectra remain unchanged, it can be concluded that these model asphaltenes are not strongly interacting with the hydrophobic C12 SAM.

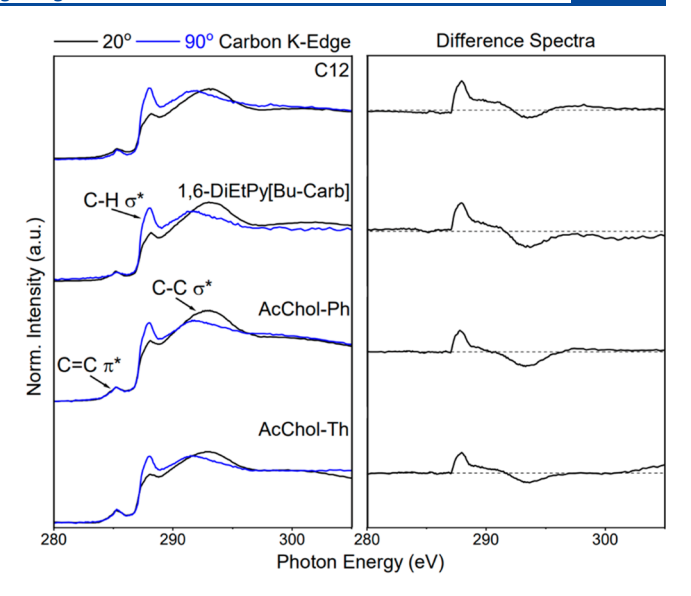


**Figure 3.** (left) NEXAFS spectra recorded at  $90^{\circ}$  and  $20^{\circ}$  X-ray incidence angles for C12 SAM with and without exposure to the asphaltene model compounds. (right) Difference between the  $90^{\circ}$  and  $20^{\circ}$  NEXAFS spectra.

XPS of Adsorbed Asphaltenes on C12 and COOH SAMs. High-resolution C 1s XPS spectra of the SAMs and adsorbed asphaltenes to the SAMs are presented in Figure 4,

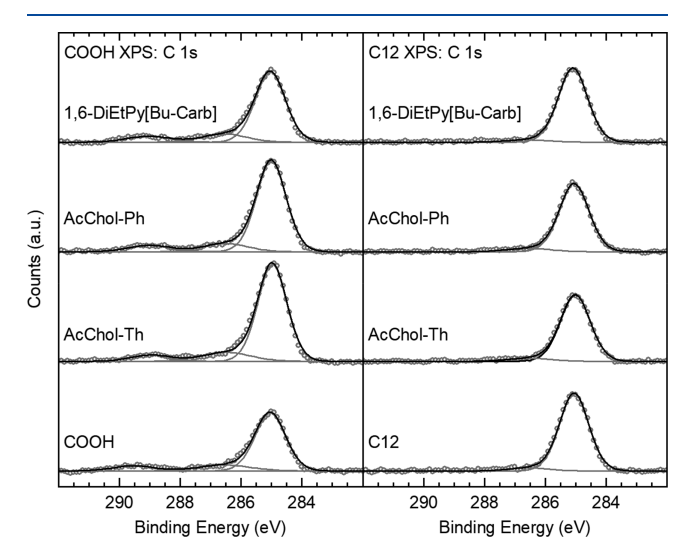


**Figure 4.** High-resolution XPS C 1s spectra (o) of carboxylic acid (COOH)-terminated (left) and methyl (C12)-terminated (right) self-assembled monolayers (SAMs) before and after the adsorption of asphaltenes AcChol-Th, AcChol-Ph, and 1,6-DiEtPy[Bu-carb]. The fit envelopes (black solid lines) and spectrum decomposition (gray solid lines) are shown. The spectra are offset for clarity.

along with corresponding fits. The C 1s spectra for the COOH SAM and COOH SAM with the adsorbed model compounds contain three distinct features, one at 285.0 eV corresponding to the C—C bonds from the SAM and asphaltenes, and higher-energy shoulders at 286.5 eV.<sup>34</sup> The shoulder can be assigned to the C—O, C—S, and C—N group. A peak near 288.5 eV can be assigned to the O—C=O terminal group.<sup>27</sup> Here, the C—O and C—S groups can be assigned directly to the SAM, while after the adsorption of the asphaltenes additional C—S and C—N bonds are added to the feature at

Table 1. XPS Determined Elemental Compositions for Asphaltenes on Methyl (C12)- and Carboxylic Acid (COOH)-Terminated SAMs

sample	C 1s atom % (std. dev. a)	O 1s atom % (std. dev.)	S 2p atom % (std. dev.)	Au 4f atom % (std. dev.)
COOH SAM	47.8 (1.0)	9.0 (0.3)	1.6 (0.5)	41.6 (1.2)
COOH + AcChol-Th	61.0 (0.9)	9.0 (0.5)	0.5 (0.5)	29.5 (0.3)
COOH + AcChol-Ph	61.9 (0.8)	8.2 (0.6)	n.d.	29.9 (0.5)
COOH + 1,6-DiEtPy[Bu-Carb]	53.3 (0.4)	9.2 (0.7)	0.8 (0.8)	36.7 (0.2)
C12 SAM	47.9 (1.0)	n.d. <sup>b</sup>	1.8 (0.6)	50.3 (0.6)
C12 + AcChol-Th	47.1 (1.2)	n.d.	0.9 (0.9)	52.0 (0.6)
C12 + AcChol-Ph	47.3 (0.7)	n.d.	1.9 (0.1)	50.8 (0.7)
C12 + 1,6-DiEtPy[Bu-Carb]	47.3 (1.2)	n.d.	1.0 (0.9)	51.7 (1.4)
<sup>a</sup> std. dev. = standard deviation. <sup>b</sup> n.d. = not detectable.				

286.5 eV, and carbon—carbon type bonds are added to the feature at 285.0 eV. The C 1s spectra for the C12 SAM and C12 SAM with adsorbed asphaltenes contain two distinct peaks, one at 285.0 eV corresponding to the C—C bonds from SAM and asphaltenes and one higher-energy shoulder at 286.5 eV.<sup>35</sup> The higher-energy feature can be assigned to just the C—S of the SAM. The S 2p spectra for each of the SAM types (Figure S1), COOH and C12, exhibit a single S 2p<sub>3/2,1/2</sub> doublet. The binding energy position of the S 2p<sub>3/2</sub> component at ca. 162.2 eV is characteristic of thiolate-type sulfur bonded to a metal such as gold.<sup>36</sup> Furthermore, there are no traces of unbonded or oxidized sulfur in the spectrum.

XPS was also used to determine the elemental compositions of the SAMs and asphaltene compounds adsorbed to the SAM surface. These data are presented in Table 1, and survey spectra are presented in Figure S2. The surface composition shows the presence of carbon, sulfur, and gold (from the underlying substrate). However, only the COOH SAM-containing samples have detectable oxygen. Furthermore, only the COOH SAM showed a change in the surface elemental composition upon exposure to asphaltene solutions. The C12 SAM remained constant for every sample, indicating no adsorption of asphaltenes to the C12 SAM surface. For the COOH SAM and adsorbed asphaltenes, AcChol-Th and AcChol-Ph showed similar atomic percent changes in C 1s and the substrate Au 4f emission, while 1,6-DiEtPy[Bu-Carb] has the least amount of C 1s of the asphaltenes.

To determine the amount of asphaltenes on the surface of the SAMs, the overlayer XPS C 1s data of the SAMs with adsorbed asphaltenes were normalized to the C 1s XPS data of just the SAMs.<sup>37</sup> This utilizes the concept of inelastic mean free path (IMFP), whereby X-rays can penetrate deep into the sample while only electrons, without energy loss, typically originating from the outermost 8 nm of a surface, are detected.<sup>38</sup> For the asphaltenes adsorbed to the SAM surface, the intensity of the Au 4f will decrease because the only source of Au 4f is from the substrate, and as the asphaltene overlayer becomes thicker, fewer emitted gold electrons will be recorded. The normalization was done by applying eq 1, and the data are recorded in Table 2. The normalized COOH SAM C 1s with adsorbed asphaltenes, which is a direct measurement of the amount of asphaltenes adsorbed to the surface of the SAMs, indicates that both the AcChol-Ph and AcChol-Th have about 58% more carbon on the surface compared to 1,6-DiEtPy[Bu-Carb], indicating that more asphaltenes are adsorbed to the SAM surface. No change in the C 1s of the C12 SAM after being in the solution of asphaltenes indicates that no asphaltene adsorption to the C12 SAM surface occurs. The effective overlayer thickness, apart from the composition

Table 2. Normalized XPS Determined Carbon Content and Calculated Layer Thicknesses of Asphaltenes on Methyl (C12)- and Carboxylic Acid (COOH)-Terminated SAMs

sample	normalized C 1s atom % (std. dev. <sup>a</sup> )	layer thickness [Å] (std. dev.)
COOH + AcChol-Th	27.1 (1.5)	7.4 (0.3)
COOH + AcChol-Ph	27.6 (1.6)	7.1 (0.3)
COOH + 1,6- DiEtPy[Bu-Carb]	11.2 (1.6)	2.7 (0.3)
C12 + AcChol-Th	-2.4 (1.7)	0
C12 + AcChol-Ph	-1.0 (1.5)	0
C12 + 1,6-DiEtPy[Bu- Carb]	-1.9 (2.1)	0

<sup>a</sup>std. dev. = standard deviation.

analysis, can be determined based off the intensities from the C 1s and Au 4f ratios using eq 2 and previously reported attenuation lengths. 22,39 Following the procedure, we obtain average thickness values for the asphaltenes adsorbed to the COOH SAM of 7.4  $\pm$  0.3 Å for AcChol-Th, 7.1  $\pm$  0.3 Å for AcChol-Ph, and  $2.7 \pm 0.3$  Å for 1,6-DiEtPy[Bu-Carb]. From this, we observe that subtle differences in molecular structure between AcChol-Ph and AcChol-Th do not significantly affect the average thickness. The schematic of asphaltene adoption can be seen in Figure 5. Both AcChol-Th and AcChol-Ph have similar dimensions, approximately 13 Å by 20 Å. Thus, for a dense upright orientation, the layer thickness measured by XPS would be either approximately 13 Å if the asphaltene was lying on its long axis or 20 Å if on the short axis. Combining the XPS results with NEXAFS, AcChol-Ph (Figure 5b) must lie on its long axis and partially penetrate into the SAM, while AcChol-Th (Figure 5c) must lie on its short axis with a nearly flat orientation to the SAM surface. The 1,6-DiEtPy[Bu-Carb] asphaltene (Figure 5d) has dimensions of approximately 11 Å by 23 Å, and thus, to satisfy the XPS layer thickness for a monolayer on the COOH SAM surface, the asphaltene must be lying very nearly parallel to the surface of the COOH SAM. The other possible configuration could be a bent structure, where the two pendant carbazole moieties can freely rotate around the butyl links of the asphaltene, and the central pyrene structure can lie parallel to the COOH SAM surface. From the NEXAFS spectra, the asphaltene ring structures were determined to have a slight preference for a perpendicular orientation. Together, this strongly supports the bent structure conformation of the asphaltene, where the central pyrene structure can lie flat on the surface of the COOH SAM, and the two pendant carbazole moieties can be perpendicular to the surface so that the XPS thickness of  $2.7 \pm 0.3$  Å is satisfied.

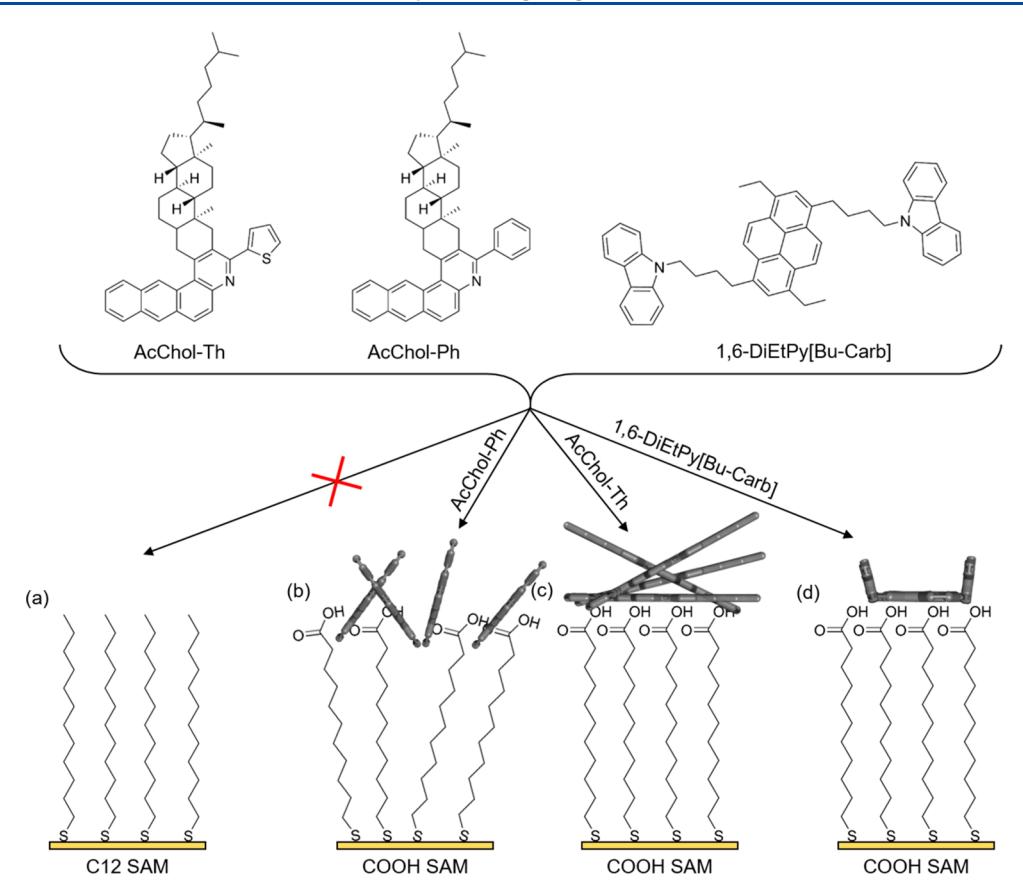


Figure 5. Simplified schematic for asphaltene adsorption onto COOH and C12 SAMs. (a) No asphaltene adsorption onto C12 SAM. (b) AcChol-Ph partially inserted into the COOH SAM and lying on its short axis. (c) AcChol-Th strongly tilted toward the surface of the COOH SAM. (d) The 1,6-DiEtPy[Bu-Carb] asphaltene has dimensions of approximately 11 Å by 23 Å, and thus, to satisfy the XPS layer thickness for a monolayer of the COOH SAM surface, the asphaltene must have a strong tilt toward the surface of the COOH SAM.

The adsorption and positioning of natural asphaltene molecules at interfaces have been debated from having large aromatic cores parallel to interfaces to molecules positioned perpendicular to the interface. 6,40 Some of this apparent discrepancy is mainly due to the large geochemical variability in composition, molecular structure, and the observation that the molecular nature of adsorbed asphaltenes is different from the asphaltenes in bulk. 41 Much interpretation has been based on interfacial tension analysis using the Gibbs-Langmuir approach estimating an average occupied area/molecule and the analogy with simple molecules. 42 The latter may, even for simple molecules, show that simple polyaromatics are not adsorbed with the aromatic sheet parallel to the water-oil interface but is positioned in some angular ordered fashion.<sup>43</sup> Likewise, asphaltenes may be positioned very differently depending on molecular architecture as reviewed by Sauerer et al.6

# CONCLUSIONS

In summary, the data allow the conclusion that model asphaltenes AcChol-Th, AcChol-Ph, and 1,6-DiEtPy[Bu-Carb] adsorb to hydrophilic COOH SAM surfaces via three different interactions, whereas asphaltene adsorption to hydrophobic C12 SAMs is not detected. Our results demonstrate the need for studying pure quasi-asphaltene constituents, as shown by AcChol-Ph, AcChol-Th, and 1,6-DiEtPy[Bu-Carb], which each have different binding motifs when bound to the model COOH SAM substrate even though

they are all, relatively speaking, from the same family of asphaltene molecules. This strongly supports the hypothesis that, with the low solubility of the asphaltenes in n-alkanes, one should expect that the dense  $\mathrm{CH}_2/\mathrm{CH}_3$  environment will have no significant repulsive interaction with the asphaltene molecules. Furthermore, our work here demonstrates how crucial it is to avoid corrosion on the metallic (often iron) well surfaces, as the presence of oxygen yields a surface that aromatic asphaltenes can easily stick to. This initial layer of asphaltenes may attract other asphaltene aggregates, creating an expensive problem for oil wells.

# ASSOCIATED CONTENT

#### Supporting Information

The Supporting Information is available free of charge at https://pubs.acs.org/doi/10.1021/acs.langmuir.1c01338.

XPS survey scans and high-resolution sulfur S 2p data (PDF)

# AUTHOR INFORMATION

#### **Corresponding Author**

Tobias Weidner — Department of Chemistry, Aarhus University, 8000 Aarhus C, Denmark; oorcid.org/0000-0002-7083-7004; Email: weidner@chem.au.dk

#### Authors

**Thaddeus W. Golbek** – Department of Chemistry, Aarhus University, 8000 Aarhus C, Denmark

- Ryan A. Faase The School of Chemical, Biological, and Environmental Engineering, Oregon State University, Corvallis, Oregon 97331, United States
- Mette H. Rasmussen Department of Chemistry, Aarhus University, 8000 Aarhus C, Denmark
- Rik R. Tykwinski Department of Chemistry, University of Alberta, Edmonton, Alberta T6G 2G2, Canada;
  orcid.org/0000-0002-7645-4784
- Jeffrey M. Stryker Department of Chemistry, University of Alberta, Edmonton, Alberta T6G 2G2, Canada;
  orcid.org/0000-0001-9568-5193
- Simon Ivar Andersen Danish Hydrocarbon Research and Technology Centre, Technical University of Denmark, Kgs. Lyngby 2800, Denmark
- Joe E. Baio The School of Chemical, Biological, and Environmental Engineering, Oregon State University, Corvallis, Oregon 97331, United States; orcid.org/0000-0002-9692-689X

Complete contact information is available at: https://pubs.acs.org/10.1021/acs.langmuir.1c01338

#### **Author Contributions**

The manuscript was written though contributions of all authors. All authors have given approval to the final version of the manuscript.

#### **Funding**

T.W. thanks the Danish Hydrocarbon Research and Technology Centre (DHRTC) for a research grant (CA\_192). T.W.G. thanks the Lundbeck Foundation (postdoc grant R322-2019-2461). R.R.T. and J.M.S. thank the Natural Sciences and Engineering Research Council of Canada (NSERC).

# **Notes**

The authors declare no competing financial interest.

# ABBREVIATIONS

XPS, X-ray photoelectron spectroscopy; C12, 1-dodecanethiol; COOH, 11-mercaptoundeconoic acid; SAM, self-assembled monolayer; GLAD, glancing angle deposition; AFM, atomic force microscopy; FT-ICR MS, Fourier transform ion cyclotron resonance mass spectrometry; IMFP, inelastic mean free path

# REFERENCES

- (1) Speight, J. G. Petroleum Asphaltenes-Part 1: Asphaltenes, resins and the structure of petroleum. *Oil Gas Sci. Technol.* **2004**, *59* (5), 467–477.
- (2) Goual, L. Petroleum asphaltenes. In *Crude oil emulsions—composition stability and characterization*; Abdul-Raouf, M. E., Ed.; IntechOpen, 2012; pp 27–42.
- (3) León, O.; Rogel, E.; Espidel, J.; Torres, G. Asphaltenes: Structural Characterization, Self-Association, and Stability Behavior. *Energy Fuels* **2000**, *14* (1), 6–10.
- (4) Acevedo, N.; Moulian, R.; Chacón-Patiño, M. L.; Mejia, A.; Radji, S.; Daridon, J.-L.; Barrère-Mangote, C.; Giusti, P.; Rodgers, R. P.; Piscitelli, V.; Castillo, J.; Carrier, H.; Bouyssiere, B. Understanding Asphaltene Fraction Behavior through Combined Quartz Crystal Resonator Sensor, FT-ICR MS, GPC ICP HR-MS, and AFM Characterization. Part I: Extrography Fractionations. *Energy Fuels* **2020**, 34 (11), 13903–13915.
- (5) Andrews, A. B.; McClelland, A.; Korkeila, O.; Demidov, A.; Krummel, A.; Mullins, O. C.; Chen, Z. Molecular Orientation of Asphaltenes and PAH Model Compounds in Langmuir—Blodgett Films Using Sum Frequency Generation Spectroscopy. *Langmuir* **2011**, 27 (10), 6049–6058.

- (6) Sauerer, B.; Stukan, M.; Buiting, J.; Abdallah, W.; Andersen, S. Dynamic Asphaltene-Stearic Acid Competition at the Oil–Water Interface. *Langmuir* **2018**, *34* (19), 5558–5573.
- (7) Toulhoat, H.; Prayer, C.; Rouquet, G. Characterization by atomic force microscopy of adsorbed asphaltenes. *Colloids Surf., A* **1994**, *91*, 267–283.
- (8) Schuler, B.; Meyer, G.; Peña, D.; Mullins, O. C.; Gross, L. Unraveling the Molecular Structures of Asphaltenes by Atomic Force Microscopy. *J. Am. Chem. Soc.* **2015**, *137* (31), 9870–9876.
- (9) Sabbaghi, S.; Shariaty-Niassar, M.; Ayatollahi, S. H.; Jahanmiri, A. Characterization of asphaltene structure using atomic force microscopy. *J. Microsc.* **2008**, *231* (3), 364–373.
- (10) Marcano, M. C.; Kim, S.; Becker, U. Surface interaction of crude oil, maltenes, and asphaltenes with calcite: An atomic force microscopy perspective of incipient wettability change. *Appl. Geochem.* **2020**, *113*, 104501.
- (11) Kamkar, M.; Natale, G. A review on novel applications of asphaltenes: A valuable waste. Fuel 2021, 285, 119272.
- (12) Schuler, B.; Zhang, Y.; Collazos, S.; Fatayer, S.; Meyer, G.; Pérez, D.; Guitián, E.; Harper, M. R.; Kushnerick, J. D.; Pena, D. Characterizing aliphatic moieties in hydrocarbons with atomic force microscopy. *Chem. Sci.* **2017**, *8* (3), 2315–2320.
- (13) Schuler, B.; Fatayer, S.; Meyer, G.; Rogel, E.; Moir, M.; Zhang, Y.; Harper, M. R.; Pomerantz, A. E.; Bake, K. D.; Witt, M.; Peña, D.; Kushnerick, J. D.; Mullins, O. C.; Ovalles, C.; van den Berg, F. G. A.; Gross, L. Heavy Oil Based Mixtures of Different Origins and Treatments Studied by Atomic Force Microscopy. *Energy Fuels* **2017**, *31* (7), 6856–6861.
- (14) Gross, L.; Schuler, B.; Pavliček, N.; Fatayer, S.; Majzik, Z.; Moll, N.; Peña, D.; Meyer, G. Atomic force microscopy for molecular structure elucidation. *Angew. Chem., Int. Ed.* **2018**, *57* (15), 3888–3908.
- (15) Zhang, Y.; Schuler, B.; Fatayer, S.; Gross, L.; Harper, M. R.; Kushnerick, J. D. Understanding the Effects of Sample Preparation on the Chemical Structures of Petroleum Imaged with Noncontact Atomic Force Microscopy. *Ind. Eng. Chem. Res.* **2018**, *57* (46), 15935–15941.
- (16) Chen, P.; Fatayer, S.; Schuler, B.; Metz, J. N.; Gross, L.; Yao, N.; Zhang, Y. The Role of Methyl Groups in the Early Stage of Thermal Polymerization of Polycyclic Aromatic Hydrocarbons Revealed by Molecular Imaging. *Energy Fuels* **2021**, 35 (3), 2224–2233.
- (17) Scott, D. E.; Schulze, M.; Stryker, J. M.; Tykwinski, R. R. *Chem. Soc. Rev.* [Online early access]. DOI: 10.1039/D1CS00048A. Published Online: July 6, **2021**, https://pubs.rsc.org/en/content/articlelanding/2021/CS/D1CS00048A.
- (18) Gray, M. R.; Tykwinski, R. R.; Stryker, J. M.; Tan, X. Supramolecular Assembly Model for Aggregation of Petroleum Asphaltenes. *Energy Fuels* **2011**, 25 (7), 3125–3134.
- (19) Schulze, M.; Scott, D. E.; Scherer, A.; Hampel, F.; Hamilton, R. J.; Gray, M. R.; Tykwinski, R. R.; Stryker, J. M. Steroid-Derived Naphthoquinoline Asphaltene Model Compounds: Hydriodic Acid Is the Active Catalyst in I2-Promoted Multicomponent Cyclocondensation Reactions. *Org. Lett.* **2015**, *17* (23), 5930–5933.
- (20) Diner, C.; Scott, D. E.; Tykwinski, R. R.; Gray, M. R.; Stryker, J. M. Scalable, Chromatography-Free Synthesis of Alkyl-Tethered Pyrene-Based Materials. Application to First-Generation "Archipelago Model" Asphaltene Compounds. *J. Org. Chem.* **2015**, *80* (3), 1719–1726.
- (21) Bednar, R. M.; Golbek, T. W.; Kean, K. M.; Brown, W. J.; Jana, S.; Baio, J. E.; Karplus, P. A.; Mehl, R. A. Immobilization of Proteins with Controlled Load and Orientation. *ACS Appl. Mater. Interfaces* **2019**, *11* (40), 36391–36398.
- (22) Apte, J. S.; Collier, G.; Latour, R. A.; Gamble, L. J.; Castner, D. G. XPS and ToF-SIMS Investigation of  $\alpha$ -Helical and  $\beta$ -Strand Peptide Adsorption onto SAMs. *Langmuir* **2010**, *26* (5), 3423–3432.
- (23) Chen, X.; Yang, Z.; Feng, S.; Golbek, T. W.; Xu, W.; Butt, H.-J.; Weidner, T.; Xu, Z.; Hao, J.; Wang, Z. How Universal Is the Wetting Aging in 2D Materials. *Nano Lett.* **2020**, *20* (8), 5670–5677.

- (24) Ton-That, C.; Shard, A. G.; Bradley, R. H. Thickness of Spin-Cast Polymer Thin Films Determined by Angle-Resolved XPS and AFM Tip-Scratch Methods. *Langmuir* **2000**, *16* (5), 2281–2284.
- (25) Siemeling, U.; Rittinghaus, S.; Weidner, T.; Brison, J.; Castner, D. COOH-terminated SAMs on gold fabricated from an azobenzene derivative with a 1,2-dithiolane headgroup. *Appl. Surf. Sci.* **2010**, 256 (6), 1832–1836.
- (26) Ballav, N.; Shaporenko, A.; Krakert, S.; Terfort, A.; Zharnikov, M. Tuning the Exchange Reaction between a Self-assembled Monolayer and Potential Substituents by Electron Irradiation. *J. Phys. Chem. C* **2007**, *111* (21), 7772–7782.
- (27) Aitchison, H.; Lu, H.; Hogan, S. W. L.; Früchtl, H.; Cebula, I.; Zharnikov, M.; Buck, M. Self-Assembled Monolayers of Oligophenylenecarboxylic Acids on Silver Formed at the Liquid–Solid Interface. *Langmuir* **2016**, 32 (37), 9397–9409.
- (28) Urquhart, S. G.; Ade, H. Trends in the Carbonyl Core (C 1S, O 1S)  $\rightarrow \pi^*C = O$  Transition in the Near-Edge X-ray Absorption Fine Structure Spectra of Organic Molecules. *J. Phys. Chem. B* **2002**, *106* (34), 8531–8538.
- (29) Witte, G.; Weiss, K.; Jakob, P.; Braun, J.; Kostov, K. L.; Wöll, C. Damping of Molecular Motion on a Solid Substrate: Evidence for Electron-Hole Pair Creation. *Phys. Rev. Lett.* **1998**, *80* (1), 121–124.
- (30) Cabarcos, O. M.; Shaporenko, A.; Weidner, T.; Uppili, S.; Dake, L. S.; Zharnikov, M.; Allara, D. L. Physical and Electronic Structure Effects of Embedded Dipoles in Self-Assembled Monolayers: Characterization of Mid-Chain Ester Functionalized Alkanethiols on Au{111}. *J. Phys. Chem. C* 2008, *112* (29), 10842–10854.
- (31) Weiss, K.; Bagus, P. S.; Wöll, C. Rydberg transitions in X-ray absorption spectroscopy of alkanes: The importance of matrix effects. *J. Chem. Phys.* **1999**, *111* (15), 6834–6845.
- (32) Stöhr, J. NEXAFS Spectroscopy; Springer-Verlag: Berlin, 1992; Vol. 25.
- (33) Baio, J. E.; Jaye, C.; Fischer, D. A.; Weidner, T. Multiplexed orientation and structure analysis by imaging near-edge X-ray absorption fine structure (MOSAIX) for combinatorial surface science. *Anal. Chem.* **2013**, *85* (9), 4307–4310.
- (34) Techane, S. D.; Gamble, L. J.; Castner, D. G. Multitechnique Characterization of Self-Assembled Carboxylic Acid-Terminated Alkanethiol Monolayers on Nanoparticle and Flat Gold Surfaces. *J. Phys. Chem. C* **2011**, *115* (19), 9432–9441.
- (35) Willey, T. M.; Vance, A. L.; van Buuren, T.; Bostedt, C.; Terminello, L. J.; Fadley, C. S. Rapid degradation of alkanethiol-based self-assembled monolayers on gold in ambient laboratory conditions. *Surf. Sci.* **2005**, *576* (1), 188–196.
- (36) Castner, D. G.; Hinds, K.; Grainger, D. W. X-ray Photoelectron Spectroscopy Sulfur 2p Study of Organic Thiol and Disulfide Binding Interactions with Gold Surfaces. *Langmuir* **1996**, *12* (21), 5083–5086.
- (37) Thome, J.; Himmelhaus, M.; Zharnikov, M.; Grunze, M. Increased Lateral Density in Alkanethiolate Films on Gold by Mercury Adsorption. *Langmuir* **1998**, *14* (26), 7435–7449.
- (38) Vickerman, J. C.; Gilmore, I. S. Surface analysis: the principal techniques; John Wiley & Sons, 2011.
- (39) Lamont, C. L. A.; Wilkes, J. Attenuation Length of Electrons in Self-Assembled Monolayers of n-Alkanethiols on Gold. *Langmuir* 1999, 15 (6), 2037–2042.
- (40) Rane, J. P.; Harbottle, D.; Pauchard, V.; Couzis, A.; Banerjee, S. Adsorption Kinetics of Asphaltenes at the Oil–Water Interface and Nanoaggregation in the Bulk. *Langmuir* **2012**, 28 (26), 9986–9995.
- (41) Andersen, S. I.; Mahavadi, S. C.; Abdallah, W.; Buiting, J. J. Infrared Spectroscopic Analysis of the Composition of an Oil/Water Interfacial Film. *Energy Fuels* **2017**, *31* (9), 8959–8966.
- (42) Rane, J. P.; Zarkar, S.; Pauchard, V.; Mullins, O. C.; Christie, D.; Andrews, A. B.; Pomerantz, A. E.; Banerjee, S. Applicability of the Langmuir Equation of State for Asphaltene Adsorption at the Oil—Water Interface: Coal-Derived, Petroleum, and Synthetic Asphaltenes. *Energy Fuels* **2015**, 29 (6), 3584–3590.
- (43) Dutta, A. K.; Salesse, C. A Spectroscopic and Epifluorescence Microscopic Study of (Hexadecanoylamino)fluorescein Aggregates at

the Air-Water Interface and in Langmuir-Blodgett Films. *Langmuir* **1997**, *13*, 5401–5408.